



Optimization of electroless Ni-Co-P coating with hardness as response parameter: A computational approach

Subhasish Sarkar ¹, Rishav Kumar Baranwal ^{1,*}, Sameer Lamichaney ¹, Jhumpa De ², Gautam Majumdar ¹

¹ Department of Mechanical Engineering, Jadavpur University, Kolkata - 700032, West Bengal, INDIA.

² Department of Mechanical Engineering, Academy of Technology, Hooghly, INDIA.

*Corresponding author: rishavbaranwal22@gmail.com

KEYWORD	ABSTRACT
Electroless Taguchi orthogonal arrays Optimize Spectroscopy Microscopy Annealed	This paper reports the effects of the coating parameters on the hardness of the coating with the application of Taguchi method. The three factors viz. concentration of Cobalt sulphate, concentration of Sodium Hypophosphite and the temperature of electroless bath with three different levels each are fitted into L ₂₇ orthogonal arrays to optimize the coating conditions. The optimized results were obtained for 10 g/L concentration of Cobalt Sulphate, 25 g/L concentration of Sodium Hypophosphite and 85°C temperature. The micro hardness of this coating was 1790 VHN _{10g} . With the help of annealing at 400°C the micro-hardness increased to 2027 VHN _{10g} . Analysis of variance was applied to find the significant factors and the interactions. It has been investigated that concentration of Cobalt Sulphate and concentration of Sodium Hypophosphite were the most significant factors in determining the hardness of the Ni-Co-P coating. Presence of different phases (Co ₂ P and Ni ₃ P) in the coating was found using X-Ray diffraction analysis and composition of the coating was investigated using Energy-dispersive X-Ray Spectroscopy (EDAX). It showed high percentage of Cobalt (13.27%) and Phosphorus (8.85%) along with Nickel. Scanning Electron Microscopy analysis was used for observing the micro-structure of the substrate, optimized coating and annealed optimized coating.

Received 24 March 2018; received in revised form 19 June 2018; accepted 26 August 2018.

To cite this article: Sarkar et al. (2018). Optimization of electroless Ni-Co-P coating with hardness as response parameter: A computational approach. Jurnal Tribologi 18, pp.81-96.

NOMENCLATURE

S/N ratio	Signal to Noise Ratio
VHN _{10g}	Vickers Hardness Number at 10 gm load
L ₂₇	set of 27 orthogonal experiments (arrays)

1.0 INTRODUCTION

Electroless Coating was first introduced by Brenner and Riddle in 1946 (Brenner and Riddell, 1947). The process deposits a uniform layer of coating over any irregular/regular geometry of the substrate. It is an autocatalytic process which requires no external energy for the initiation of the process. Electroless coatings has applications which enables it to be used in industries (Goel et al., 2016; Djokic and Cavallotti, 2010). The reason for this widespread use of Ni-P coatings is its high corrosion resistance, hardness and good anti-wear rates (Allen and Vandersande, 1982; Vitry et al., 2012; Zhang et al., 2008; Georgiza et al., 2013; Narayanan et al., 2006). However, with time the desire for better properties has increased which enabled the researchers to use a third metal (W, Cu, Co, Sn, etc.) (Liu et al., 2009; Eltoun, 2016; Huang et al., 2007; Georgieva and Armyanov, 2007; Aixiang et al., 2005) or compounds like ZrO₂, TiO₂, Al₂O₃, SiC (Song et al., 2007; Chen et al., 2010; Sharma and Singh, 2013; Jiaqiang et al., 2006). These third elements/compounds not only enhance the mentioned properties but also introduces new properties like hydrophobicity, magnetism, electromagnetic shielding and lubrication (Zhu and Jin, 2007; Zhang, 2008; Gao et al., 2007).

One of the prime properties which has proved to be of importance in successful applications is hardness. Hardness of an electroless Nickel coating can be increased by the addition of Phosphorus (Sudagar et al., 2013). However, it has been shown that the hardness of the coating increases with decreasing Phosphorus content (Ashtiani et al., 2017). Hence, for an optimum amount of Phosphorus, a maximum value of hardness can be obtained. The hardness can be increased drastically by annealing the coating at 400°C (Staia et al., 1996). However, the hardness can also be increased by introduction of a third element, which in this case is Cobalt (Aal et al., 2008). Cobalt increases the anti-corrosion properties of the coating and at the same time introduces magnetism and increases electromagnetic shielding of the coating (Gao et al., 2007; Seifzadeh and Hollagh, 2014).

The aim of this research is to improve the hardness of the Copper substrate by coating it electrolessly with Ni-Co-P coating and find the optimal coating conditions for the proper hardness of the coating. There is a definite need of optimization in almost every field in order to provide proper usage of initial materials and conditions to produce a product of superior quality (Sheikholesami and Shehzad, 2018; Sheikholesami and Rokni, 2018). L₂₇ orthogonal arrays has been used in Taguchi to investigate the optimal design parameters. Analysis of Variance has been applied to this to find the significance of each factors and their interaction with each other in the hardness of the coating. Annealing of the optimized Ni-Co-P coating was done at 400°C to increase the hardness. Scanning Electron Microscope was used to find the surface morphology of the substrate, optimized coating and the annealed optimized coating while X-Ray Diffraction (XRD) was used to find the presence of different phases in the coating. Energy dispersive X-Ray Spectroscopy (EDAX) was done along with XRD to find the percentage of each element in the coating.

2.0 MATERIALS AND METHODS

2.1 Coating preparation

In this experiment Copper strips of 2×1.5 mm² from a Copper foil having a thickness of 0.1 mm. For proper and effective deposition of the coating the substrate needs to be prepared properly. The substrate has undergone pre-treatment in order to remove any possible layers of oxides, hydrocarbons. For cleaning, the substrate was first rinsed with distilled water for 2 minutes, followed by cleaning in 25% dilute HCl solution for 10 minutes at room temperature. The substrate was finally rinsed in distilled water for 2 minutes at room temperature. Some metals like Copper require activation process for the initiation of the electroless deposition (Flis and Duquette, 1984; Roahn et al., 2002; Xiang et al., 2001). Copper has also proved to be a very good alternative of aluminium, as a substrate, because aluminium has low electrical resistance and low susceptibility when compared to Copper (Rohan et al., 2002). Palladium Chloride solution is used as an activator. The substrate is fully immersed in its solution at 55°C for 8-10 seconds. The substrate was finally ready after rinsing the substrate in distilled water for some time. The substrate was then transferred into the electroless bath and a thin bright layer of Ni-Co-P coating was deposited in 1 hour. The electroless bath's composition is shown in Table 1.

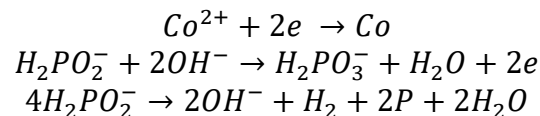
Table 1: Bath composition.

Bath Composition	Reagents	g/L
Nickel Source	NiSO ₄ .6H ₂ O	5
Cobalt Source	CoSO ₄	10, 15, 20
Reducing Agent	NaH ₂ PO ₄	20, 25, 30
Complexing Agent	Na ₃ C ₆ H ₅ O ₇ .2H ₂ O	15
Buffering Agent	(NH ₄) ₂ SO ₄	10

The operating conditions were:

pH: 5; Temperature: 80°C/ 85°C/ 90°C; Deposition time: 60 minutes; Bath Volume: 250mL; Stirring Speed: 500-600 rpm.

The reducing agent, Sodium Hypophosphite, reduces the Nickel ions provided by Nickel Sulphate Hexahydrate. The complexing reagent, Trisodium Citrate Dihydrate, formed metastable nickel complexes which allows the reaction to slow down and reach a feasible state. The buffering agent, Ammonium Sulphate, tries to maintain the pH of the solution at 5. The following reaction took place in the deposition of Ni-Co-P coating over Cu substrate:



2.2 Design of experiment

It is an effective tool to analyse the response variable. The response variable for our case is hardness of the coating. Hardness depends on the various bath parameters like the concentration of Nickel Sulphate Hexahydrate, concentration of Cobalt Sulphate, concentration of Sodium hypophosphite, concentration of complexing agent, pH of the solution and the temperature of the

bath. Out of these parameters we chose the concentration of the reducing agent, concentration of Cobalt Sulphate and the temperature of the bath as the varying properties or factors on which the hardness of the coating will vary. Each factor has three different levels, shown in Table 2, which describes the different bath conditions in which coating was done.

Table 2: Factors and their respective levels.

Design Factors	Level		
	1	2	3
Concentration of Cobalt Sulphate (A) in g/L	10	15	20
Concentration of Sodium Hypophosphite (B) in g/L	20	25	30
Temperature of the bath in °C	80	85	90

We applied the L_{27} orthogonal arrays (3x3) for evaluation of the optimal result with minimum experimental time and maximum concluding information. L_{27} orthogonal arrays consists of 13 columns and 27 rows as shown in table 3, where each column represents the factors and their interactions and each row represented the experiment. Orthogonal arrays determines the main effects and the interaction effects of the parameters with the use of minimum number of experiments. A minimum of 27 experiments has been done on the basis of number of factors and the number of levels. Analysis of Variance (ANOVA) was performed on the factors and their interaction with each other to find the effective factors and the effective interactions based on their p-values.

2.3 Response variable

The response variable in the study was the hardness of the Ni-Co-P coating. It was a single response optimisation process where the three factors were concentration of Cobalt Sulphate (A), concentration of Sodium Hypophosphite (B) and the temperature of the bath (C).

2.4 Hardness measurement

The present study investigated the hardness of Ni-Co-P coating which was deposited over soft Copper strips electrolessly. The indentation depth should be 10-20% of the coating thickness in order to avoid the substrate's effect on hardness. The loading and unloading was done for 15 seconds each using a Vickers indenter. The indenter had 136° at the tip. The microhardness was measured by applying 10 gram load on the coating. The hardness for each experiment has been shown in Table 4.

2.5 Coating's characterisation

The coating's surface morphology was done using Scanning Electron Microscopy (SEM) on the SOF software in the JEOL-Jsm7610F machine and the XRD analysis was done to find the phases present in the coating using same software on the same machine. EDAX was done to find the surface composition in AZTEC software using OXFORD X-max 50 machine.

Table 3: Factors' design.

No.	[1]	[2]	[3]	[4]	[5]	[6]	[7]	[8]	[9]	[10]	[11]	[12]	[13]
1	1	1	1	1	1	1	1	1	1	1	1	1	1
2	1	1	1	1	2	2	2	2	2	2	2	2	2
3	1	1	1	1	3	3	3	3	3	3	3	3	3
4	1	2	2	2	1	1	1	2	2	2	3	3	3
5	1	2	2	2	2	2	2	3	3	3	1	1	1
6	1	2	2	2	3	3	3	1	1	1	2	2	2
7	1	3	3	3	1	1	1	3	3	3	2	2	2
8	1	3	3	3	2	2	2	1	1	1	3	3	3
9	1	3	3	3	3	3	3	2	2	2	1	1	1
10	2	1	2	3	1	2	3	1	2	2	1	2	3
11	2	1	2	3	2	3	1	2	3	3	2	3	1
12	2	1	2	3	3	1	2	3	1	1	3	1	2
13	2	2	3	1	1	2	3	2	3	3	3	1	2
14	2	2	3	1	2	3	1	3	1	1	1	2	3
15	2	2	3	1	3	1	2	1	2	2	2	3	1
16	2	3	1	2	1	2	3	3	1	1	2	3	1
17	2	3	1	2	2	3	1	1	2	2	3	1	2
18	2	3	1	2	3	1	2	2	3	3	1	2	3
19	3	1	3	2	1	3	2	1	3	3	1	3	2
20	3	1	3	2	2	1	3	2	1	1	2	1	1
21	3	1	3	2	3	2	1	3	2	2	3	2	3
22	3	2	1	3	1	3	2	2	1	1	3	2	1
23	3	2	1	3	2	1	3	3	2	2	1	3	2
24	3	2	1	3	3	2	1	1	3	3	2	1	3
25	3	3	2	1	1	3	2	3	2	2	2	1	3
26	3	3	2	1	2	1	3	1	3	3	3	2	1
27	3	3	2	1	3	2	1	2	1	1	1	3	2

3.0 RESULTS AND DISCUSSION

3.1 Analysis of signal to noise ratio

Signal to Noise ratio (S/N) is the ratio of the valuable information to irrelevant data. The more positive the value of S/N the better the quality. Taguchi method uses S/N ratio to investigate the performance of the coating. The S/N ratio can be applied in three different ways for checking the performance. There are:

- Lower the better
- Nominal the best
- Larger the better

Higher the hardness of the coating, better the performance of the coating. So we applied 'larger the better' S/N ratio to find the optimal coating parameters. S/N ratio for larger the better is given by:

$$S / N = -10 \log_{10} \left(\frac{\sum \frac{1}{y^2}}{n} \right)$$

Where y is the measured hardness and n is the number of the experiment. S/N ratio for each level has been shown in Table 5.

Table 4: Hardness of each coating.

Cobalt Sulphate(A) in g/L	Sodium Hypophosphite(B) in g/L	Temperature of Bath(C) in °C	Harndess (VHN_{10 g})
10	20	80	1196
10	20	85	1250
10	20	90	1120
10	25	80	1860
10	25	85	1790
10	25	90	1803
10	30	80	1209
10	30	85	1150
10	30	90	1193
15	20	80	1204
15	20	85	1296
15	20	90	1250
15	25	80	1050
15	25	85	1107
15	25	90	1103
15	30	80	1556
15	30	85	1583
15	30	90	1496
20	20	80	1304
20	20	85	1357
20	20	90	1320
20	25	80	1075
20	25	85	970
20	25	90	996
20	30	80	1007
20	30	85	983
20	30	90	1056

Table 5: Response table for S/N ratio (larger is better).

Level	A	B	C
1.	62.71	61.95	61.78
2.	62.14	62.00	62.41
3.	60.89	61.78	61.54
Delta	1.82	0.21	0.87
Rank	1	3	2

The delta corresponds to the difference in maximum and minimum S/N value of levels in each factor. The rank was then designated based on the delta value. The highest S/N value of the level in the each factor corresponds to the optimal level of that factor. Thus we can clearly determine from Table 5 that the optimal bath parameters were A1B2C2, which is the 5th experiment and the corresponding hardness number of the experiment is 1790 VHN_{10g}. The main effects plot for S/N ratio also explains the same thing in Figure 1.

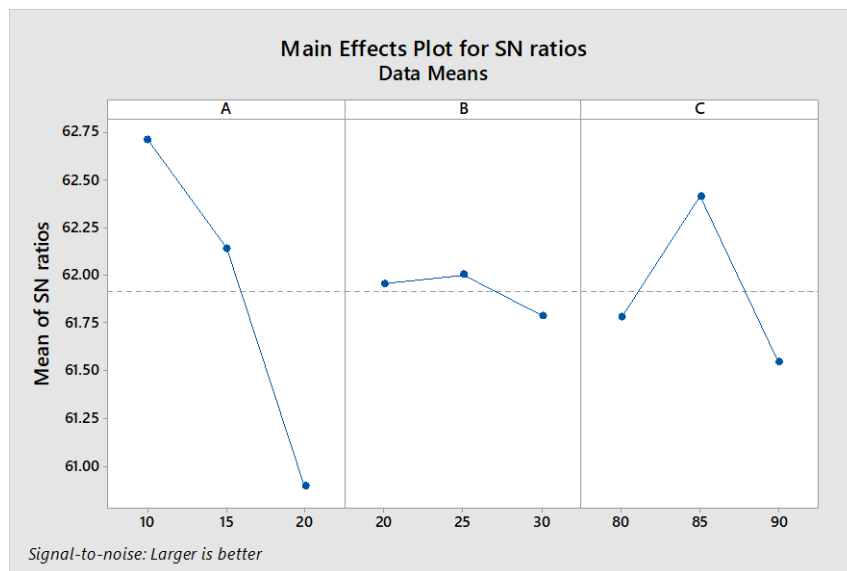


Figure 1: Main effects plot for S/N ratio.

The main effects of hardness plot (Figure 2) can be interpreted to find which factors play a more significant term in determining the hardness of the coating. The factors having the plot close to the mean line or the horizontal line will have the no significant effect on the hardness. Thus, from Figure 2 we can conclude that factor C (temperature of the bath) had no significant effect on hardness while the factors A (concentration of cobalt sulphate) and B (concentration of Sodium Hypophosphite) played a significant role in determining the hardness of the electroless coatings.

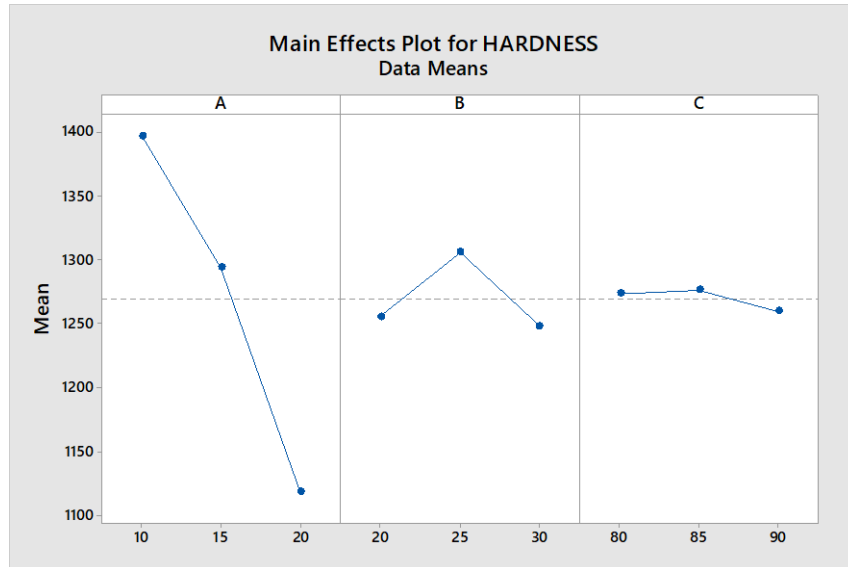


Figure 2: Main effects plot for hardness.

The interaction between the factors has been shown in Figures 3-5. From the interaction plot we can interpret whether interaction has taken place between the two factors or not. If the lines are parallel to each other then it indicates no interaction has taken place between the factors while if the lines are inclined to each other then it suggests that some interaction has taken place. If intersection takes place between the lines then it suggests strong interaction has taken place between the two factors. From figure 3-5 it can be observed that the interaction between AxB was very strong while the interaction between AxC and BxC were not that significant.



Figure 3: Interaction between A and B.

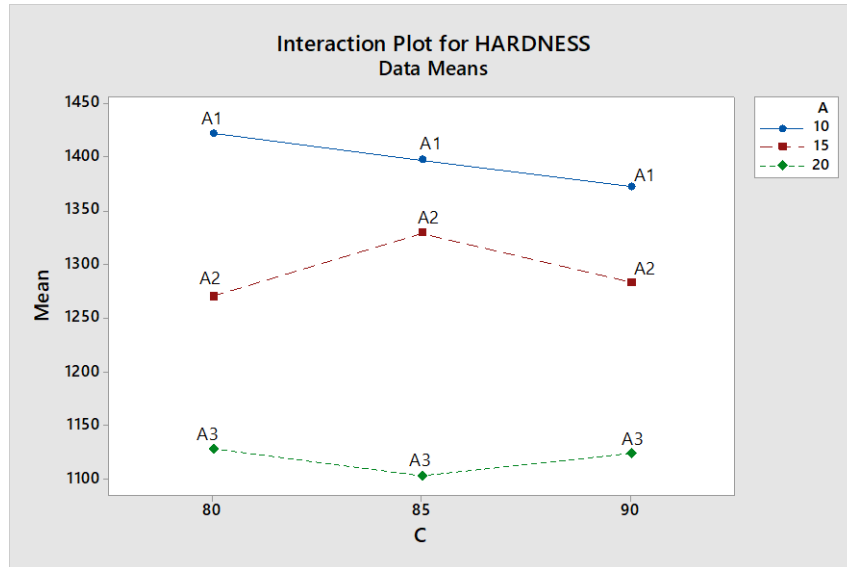


Figure 4: Interaction between A and C.

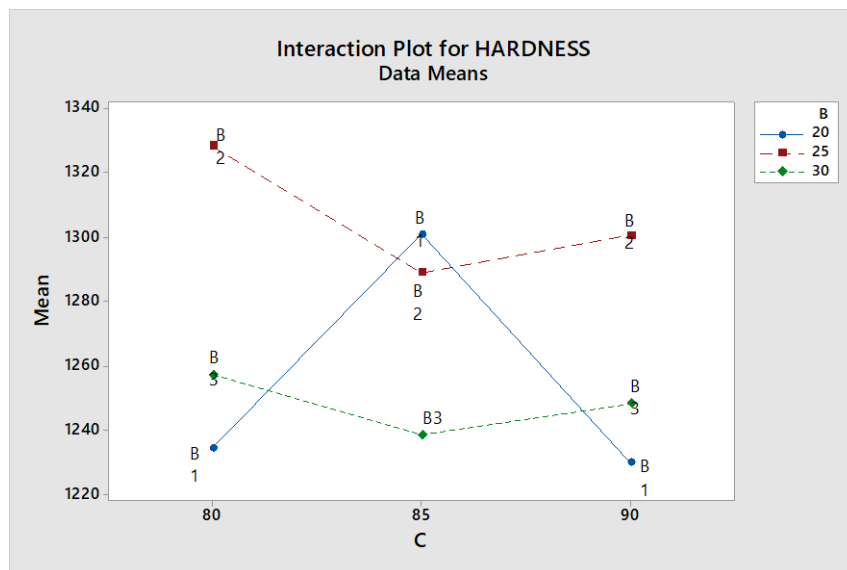


Figure 5: Interaction between B and C.

3.2 Analysis of variance (ANOVA)

It is a very good tool to conclude about the factors and their interactions. The ANOVA results are shown in Table 6.

Table 6: ANOVA results

Source	Degree of freedom	Sum of Squares	Mean Square	F ratio	p-Value
A	2	16616	8308	5.49	0.032
B	2	522232	261116	172.52	0.000
C	2	5634	2817	1.86	0.217
A*B	4	1298345	324586	214.45	0.000
A*C	4	9072	2268	1.50	0.290
B*C	4	11020	2755	1.82	0.218
ERROR	8	12109	1514		
TOTAL	26	1705805			

In Table 6, *F* ratio is the ratio of regression mean square to mean square error. The value of *F* ratio signifies the effect of each factor. The *p*-value is significant in determining whether the evidence we have in order to reject the null hypothesis is strong or weak. If the *p*-value is less than 0.05 then we have strong evidence to reject the null hypothesis and claim that the factors/interactions between factors are significant in determining the response (micro-hardness) of the coatings. Thus, the factors A (Cobalt Sulphate) and B (Sodium Hypophosphite) and the interaction between A and B have *p* value less than 0.05 and thus they are significant in determining the hardness of the coating.

3.3 Microstructural and composition study

Figure 6 show the SEM micrographs of the Copper substrate. The SEM analysis reveals the elongated grains present in the copper sample after the surface preparation.

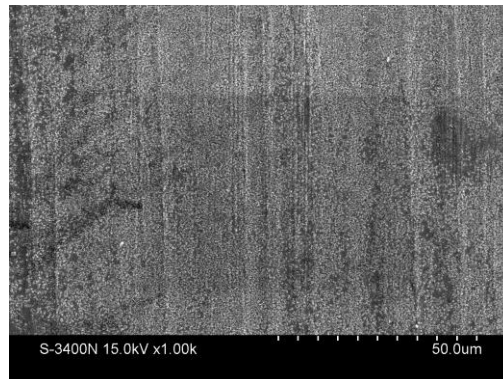


Figure 6: SEM image of the Copper substrate coating.

Figure 7 shows the FESEM image of the as-deposited coating. It shows that the thickness of the as-deposited coating was 1.94µm.

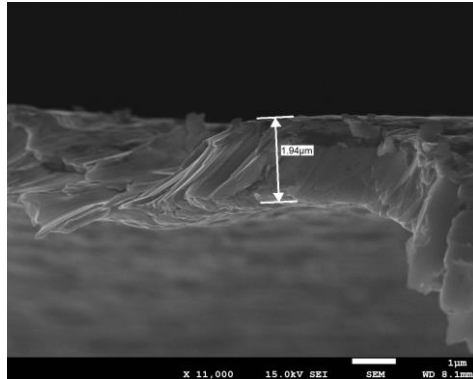


Figure 7: FESEM image of the as-deposited Ni-Co-P coating.

Figure 8 shows the SEM of the as-deposited optimized Ni-Co-P coating. The SEM analysis shows the presence of coarse nodular structure of optimized Ni-Co-P coating. The smaller black spots reveal the presence of Bakelite which has been occupied in the smaller holes (Bakelite is used as a thermosetting material while mounting the coated sample for testing hardness). This shows that the coating is porous.

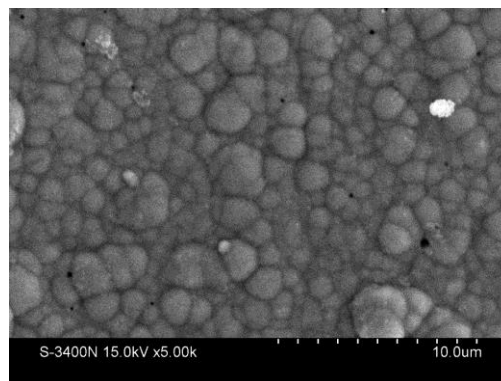


Figure 8: SEM image of the optimized Ni-Co-P coating.

Figure 9 shows the SEM image of the annealed optimized Ni-Co-P coating at 400°C. After annealing it has been found that the grain boundary has been distorted. The XRD analysis showed the presence of Ni₃P complex in the matrix. The Ni₃P complex is hard and its presence increases the hardness of the optimized coating to 2027 VHN_{10g}. The bigger nodular structures of the coating reduced to a smaller nodules due to annealing. Annealing is done to increase the hardness of the coating at the expense of the microstructure. Figure 9 SEM image of the annealed optimized Ni-Co-P coating

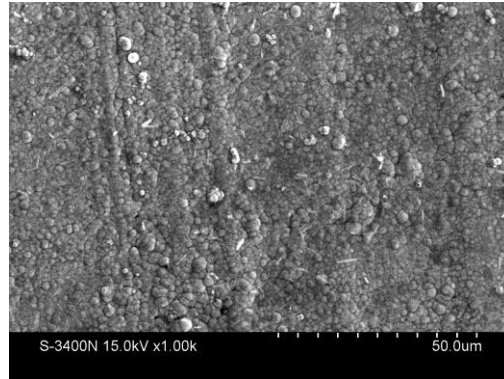


Figure 9: SEM Image of Annealed and optimized coating at 400°C.

The XRD analysis was done to find out the phases present in the coating. The presence of two phases was clearly shown from Figure 10. The XRD analysis shows peaks of Ni_3P at 43.3° and Co_2P at 50.5° .

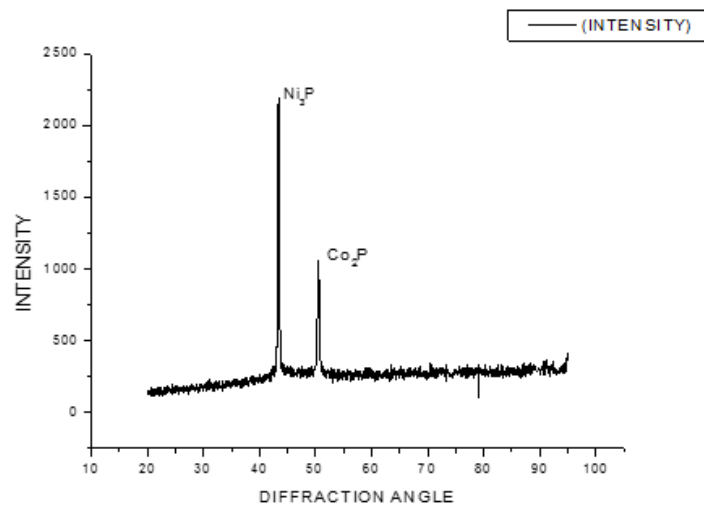


Figure 10: XRD pattern of as deposited Ni-Co-P coating.

The XRD analysis was done for the optimized sample and the presence of phases Ni_3P and Co_2P were detected as shown in Figure 11. The phases was found to shift to the right of the diffraction angle.

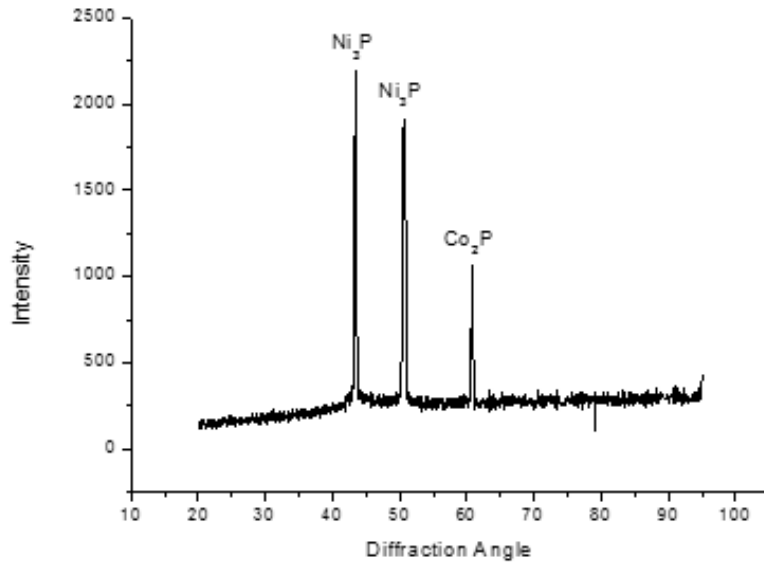


Figure 11: XRD of the annealed optimized Ni-Co-P coating at 400°C.

EDAX analysis calculates the percentage of elements in the coating. The EDAX analysis of the as-deposited optimized Ni-Co-P coating is shown in Figure 12 and the percentage of the elements are shown in the Table 7.

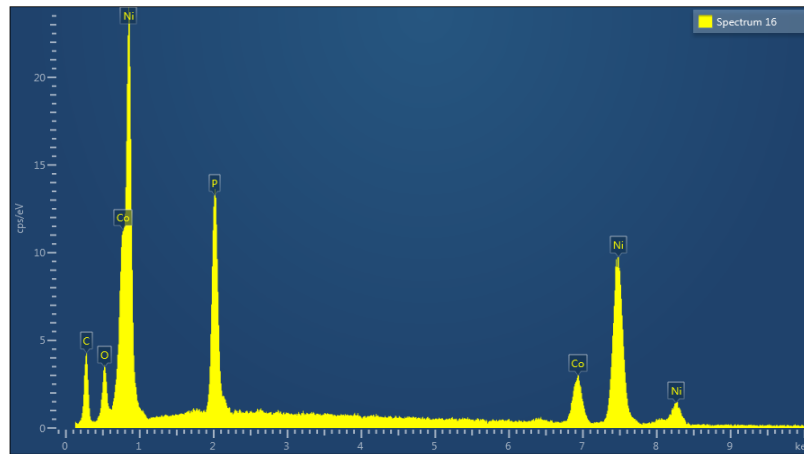


Figure 12: EDAX spectra of the as-deposited Ni-Co-P coating.

Table 7: Weight Percentage of the elements in the coating.

	Element	Weight Percentage
1	Nickel	60.02
2	Cobalt	13.27
3	Phosphorus	8.85
4	Carbon	15.01
5	Oxygen	2.86

The percentage of Phosphorus is such that it belongs to the category of coatings where high percentage of Phosphorus is present. Previous research studies claim that higher Phosphorus content coatings have good resistance to corrosion (Narayanan et al., 2006; Sahoo and Das, 2011) in the as-deposited form.

CONCLUSIONS

Taguchi Method with L_{27} orthogonal arrays was successfully applied to the experiment to find the optimized result. The optimum result from Taguchi was found out to be A1B2C2 which had a hardness of 1790 VHN_{10g}. The hardness of the optimal parameter increased by 125.72% of the substrate hardness, which was 793 VHN_{10mg}. The high hardness of the coating may be attributed due to the presence of Ni₃P phase and the use of the third element: Cobalt. The annealed optimized coating marked the hardness number at 2027 VHN_{10 g}. The increase in the hardness can be attributed to the increase in Ni₃P phase in the matrix. ANOVA analysis showed that the concentration of the Cobalt Sulphate and concentration of Sodium Hypophosphite were significant factors in contributing to hardness. The interaction between A and B also held significance in determining the hardness of the coating. SEM analysis showed the presence of different grain structures i.e. elongated grains in Cu substrate while larger and smaller nodules in un-annealed optimized and annealed optimized coating respectively. Porous nature of this coating was revealed by this analysis. EDAX analysis showed the presence of 13.27% Cobalt and 8.85% Phosphorus. The XRD analysis revealed the presence of Ni₃P phase and Co₂P phase.

REFERENCES

- Aal, A. A., Shaaban, A., & Hamid, Z. A. (2008). Nanocrystalline soft ferromagnetic Ni-Co-P thin film on Al alloy by low temperature electroless deposition. *Applied Surface Science*, 254(7), 1966-1971.
- Aixiang, Z., Weihao, X., & Jian, X. (2005). Electroless Ni-Co-P coating of cenospheres using [Ag(NH₃)₂]⁺ activator. *Materials Letters*, 59(4), 524-528.
- Allen, R. M., & VanderSande, J.B. (1982). The structure of electroless Ni-P films as a function of composition. *Scripta Metallurgica*, 16, 1161-1164.
- Ashtiani, A. A., Faraji, S., Iranagh, S. A., & Faraji, A. H. (2017). The study of electroless Ni-P alloys with different complexing agents on Ck45 steel substrate. *Arabian Journal of Chemistry*, 10, S1541-S1545.
- Brenner, A., & Riddell, G. E. (1947). Deposition of nickel and cobalt by chemical reduction. *Journal of Research of the National Bureau of Standards*, 39, 385-395.
- Chen, W., Gao, W., & He, Y. (2010). Sol-enhanced triple-layered Ni-P-TiO₂ composite coatings. *Journal of sol-gel science and technology*, 55(2), 187-190.
- Djokić, S. S., & Cavallotti, P. L. (2010). Electroless deposition: Theory and applications. In *Electrodeposition* (pp. 251-289). Springer, New York, NY.
- Eltoum, M. A. (2016). Electroless and Corrosion of Nickel-Phosphorus-Tungsten Alloy. *The Journal of Middle East and North Africa Sciences*, 10(3907), 1-9.
- Flis, J., & Duquette, D. J. (1984). Initiation of Electroless Nickel Plating on Copper, Palladium - Activated Copper, Gold, and Platinum. *Journal of The Electrochemical Society*, 131(2), 254-260.

- Gao, Y., Huang, L., Zheng, Z. J., Li, H., & Zhu, M. (2007). The influence of cobalt on the corrosion resistance and electromagnetic shielding of electroless Ni-Co-P deposits on Al substrate. *Applied Surface Science*, 253(24), 9470-9475.
- Georgieva, J., & Armyanov, S. (2007). Electroless deposition and some properties of Ni-Cu-P and Ni-Sn-P coatings. *Journal of Solid State Electrochemistry*, 11(7), 869-876.
- Georgiza, E., Novakovic, J., & Vassiliou, P. (2013). Characterization and corrosion resistance of duplex electroless Ni-P composite coatings on magnesium alloy. *Surface and Coatings Technology*, 232, 432-439.
- Goel, V., Anderson, P., Hall, J., Robinson, F., & Bohm, S. (2016). Application of Co-Ni-P Coating on Grain-Oriented Electrical Steel. *IEEE transactions on magnetics*, 52(4), 1-8.
- Huang, Y., Shi, K., Liao, Z., Wang, Y., Wang, L., & Zhu, F. (2007). Studies of electroless Ni-Co-P ternary alloy on glass fibers. *Materials letters*, 61(8-9), 1742-1746.
- Jiaqiang, G., Lei, L., Yating, W., Bin, S., & Wenbin, H. (2006). Electroless Ni-P-SiC composite coatings with superfine particles. *Surface and Coatings Technology*, 200(20-21), 5836-5842.
- Liu, W. L., Hsieh, S. H., Chen, W. J., & Hsu, Y. C. (2009). Growth behavior of electroless Ni-Co-P deposits on Fe. *Applied Surface Science*, 255(6), 3880-3883.
- Narayanan, T. S., Baskaran, I., Krishnaveni, K., & Parthiban, S. (2006). Deposition of electroless Ni-P graded coatings and evaluation of their corrosion resistance. *Surface and Coatings Technology*, 200(11), 3438-3445.
- Rohan, J. F., O'Riordan, G., & Boardman, J. (2002). Selective electroless nickel deposition on copper as a final barrier/bonding layer material for microelectronics applications. *Applied Surface Science*, 185(3-4), 289-297.
- Sahoo, P., & Das, S. K. (2011). Tribology of electroless nickel coatings—a review. *Materials & Design*, 32(4), 1760-1775.
- Seifzadeh, D., & Hollagh, A. R. (2014). Corrosion resistance enhancement of AZ91D magnesium alloy by electroless Ni-Co-P coating and Ni-Co-P-SiO₂ nanocomposite. *Journal of Materials Engineering and Performance*, 23(11), 4109-4121.
- Sharma, A., & Singh, A. K. (2013). Electroless Ni-P and Ni-P-Al₂O₃ nanocomposite coatings and their corrosion and wear resistance. *Journal of Materials Engineering and Performance*, 22(1), 176-183.
- Sheikholeslami, M., & Rokni, H. B. (2018). Magnetic nanofluid flow and convective heat transfer in a porous cavity considering Brownian motion effects. *Physics of Fluids*, 30(1), 012003.
- Sheikholeslami, M., & Shehzad, S. A. (2018). CVFEM simulation for nanofluid migration in a porous medium using Darcy model. *International Journal of Heat and Mass Transfer*, 122, 1264-1271.
- Song, Y. W., Shan, D. Y., & Han, E. H. (2007). High corrosion resistance multilayer nickel coatings on AZ91D magnesium alloys. *Surface Engineering*, 23(5), 329-333.
- Staia, M. H., Castillo, E. J., Puchi, E. S., Lewis, B., & Hintermann, H. E. (1996). Wear performance and mechanism of electroless Ni-P coating. *Surface and coatings Technology*, 86, 598-602.
- Sudagar, J., Lian, J., & Sha, W. (2013). Electroless nickel, alloy, composite and nano coatings—A critical review. *Journal of Alloys and Compounds*, 571, 183-204.
- Vitry, V., Sens, A., Kanta, A. F., & Delaunois, F. (2012). Wear and corrosion resistance of heat treated and as-plated Duplex NiP/NiB coatings on 2024 aluminum alloys. *Surface and Coatings Technology*, 206(16), 3421-3427.
- Xiang, Y., Hu, W., Liu, X., Zhao, C., & Ding, W. (2001). Initial deposition mechanism of electroless nickel plating on magnesium alloys. *Transactions of the IMF*, 79(1), 30-32.

- Zhang, S., Zhou, J., Guo, B., Zhou, H., Pu, Y., & Chen, J. (2008). Friction and wear behavior of laser cladding Ni/hBN self-lubricating composite coating. *Materials Science and Engineering: A*, 491(1-2), 47-54.
- Zhang, W. X., Jiang, Z. H., Li, G. Y., Jiang, Q., & Lian, J. S. (2008). Electroless Ni-P/Ni-B duplex coatings for improving the hardness and the corrosion resistance of AZ91D magnesium alloy. *Applied Surface Science*, 254(16), 4949-4955.
- Zhu, L., & Jin, Y. (2007). A novel method to fabricate water-soluble hydrophobic agent and super-hydrophobic film on pretreated metals. *Applied Surface Science*, 253(7), 3432-3439.